Draft version April 28, 2016
Preprint typeset using LaTeX style emulateapj v. 5/2/11

arXiv:1601.02734v2 [astro-ph.HE] 27 Apr 2016

SEARCH FOR HIGH ENERGY GAMMA-RAY EMISSION FROM TIDAL DISRUPTION EVENTS WITH THE *FERMI* LARGE AREA TELESCOPE

Fang-Kun Peng[1,2], Qing-Wen Tang[3] and Xiang-Yu Wang[1,2]

Draft version April 28, 2016

ABSTRACT

Massive black holes at galaxy center may tear apart a star when the star passes occasionally within the disruption radius, which is the so-called tidal disruption event(TDE). Most TDEs radiate with thermal emission resulted from the accretion disk, but three TDEs have been detected in bright non-thermal X-ray emission, which is interpreted as arising from the relativistic jets. Search for high-energy gamma-ray emission from one relativistic TDE (Swift J164449.3+573451) with the *Fermi* Large Area Telescope (LAT) has yielded non-detection. In this paper, we report the search for high energy emission from the other two relativistic TDEs (Swift J2058.4+0516 Swift J1112.2-8238) during the flare period. No significant GeV emission is found, with an upper limit fluence in LAT energy range being less than 1% of that in X-rays. Compared with gamma-ray bursts (GRBs) and blazars, these TDEs have the lowest flux ratio between GeV emission and X-ray emission. The non-detection of high-energy emission from relativistic TDEs could be due to that the high-energy emission is absorbed by soft photons in the source. Based on this hypothesis, upper limits on the bulk Lorentz factors, $\Gamma \lesssim 30$, are then obtained for the jets in these TDEs. We also search for high-energy gamma-ray emission from the nearest TDE discovered to date, ASASSN-14li. No significant GeV emission is found and an upper limit of $L(0.1-10\mathrm{GeV}) \leq 4.4\times10^{42}$ erg s^{-1} (at 95% confidence level) is obtained for the first 10^7 s after the disruption.

Subject headings: gamma-ray: galaxies–X-ray: flare–radiation mechanisms: non-thermal

1. INTRODUCTION

TDE is an astronomical phenomenon that occurs when a star gets too close to a supermassive black hole in the galaxy center and is disrupted by the tidal force of the black hole. Part of stellar material is bound and accreted by the central black hole, resulting in a bright optical, UV and soft X-ray emission (Rees 1988; Lodato et al. 2015, and references therein). There are growing number of candidate TDEs being discovered in soft X-ray, ultraviolet and optical surveys, see Komossa (2015) for a recent review. Recently, three unusual TDE candidates are discovered by *Swift*, i.e. Swift J164449.3+573451 Swift J2058.4+0516 Swift J1112.2-8238 (hereafter Sw J1644+57, Sw J2058+05 and Sw J1112-82 for short respectively), which have very bright non-thermal hard X-ray and radio emissions (Burrows et al. 2011; Bloom et al. 2011; Zauderer et al. 2011; Krimm et al. 2011; Cenko et al. 2012; Krimm et al. 2011; Brown et al. 2015). The luminous non-thermal X-ray and radio emissions are thought to be produced by relativistic jets (Bloom et al. 2011; Levan et al. 2011; Burrows et al. 2011; Zauderer et al. 2011; Metzger et al. 2012; Cao & Wang 2012; Wang et al. 2014; Liu et al. 2015). Sw J1644+57 shows a highly variable light curve in X-rays, as observed by X-Ray Telescope (XRT) onboard *Swift*. At redshift $z = 0.354$, the isotropic luminosity of the X-ray emission is as high as $10^{48}-10^{49}$ erg s^{-1}. Sw J2058+05 exhibits a luminous, long-lived X-ray outburst with an isotropic peak luminosity of 3×10^{47}erg s^{-1} (at redshift $z = 1.1853$). Its total isotropic energy (0.3-10 keV) on timescale of the first two months amounts to 10^{54} erg. Sw J1112-82 was initially also discovered by Swift/BAT (Burst Alert Telescope) in June 2011 as an unknown, long-lived (order of days) γ-ray transient source. It exhibits a similar bright X-ray flare and its position is consistent with the nucleus of a faint galaxy at $z = 0.89$ (Brown et al. 2015). The peak X/γ-ray luminosity of Sw J1112-82 exceeds 10^{47}erg s^{-1}.

The non-thermal X-ray emission is thought to be produced by synchrotron radiation of relativistic electrons. One would naturally expect inverse-Compton scattering emission from the same electrons, which may produce high-energy gamma-ray emission. As the three TDEs with relativistic jets emit a total isotropic energy of about 10^{54} erg in X-ray band, comparable to or even larger than that in the GRB prompt emission and blazars flares, one would expect the high-energy gamma-ray emission detectable by *Fermi*/LAT. Motivated by this, we search for high-energy gamma-ray emission from these three relativistic TDEs.

ASASSN-14li is a normal optically-discovered TDE at distance of about 90 Mpc (Holoien et al. 2016). Transient radio emission has been detected from this event and modeling of the radio emission gives a kinetic energy of 10^{48} erg in a non-relativistic or mildly relativistic outflow (Alexander et al. 2015; van Velzen et al. 2015). The relativistic electrons producing radio emission may in principle also produce high-energy gamma-ray emission, although the flux level depends on the energy of these electrons and the strength of the magnetic field. It is also proposed that the unbound debris after the dis-

[1] School of Astronomy and Space Science, Nanjing University, Nanjing 210093, China; xywang@nju.edu.cn
[2] Key laboratory of Modern Astronomy and Astrophysics (Nanjing University), Ministry of Education, Nanjing 210093, China
[3] School of Science, Nanchang University,Nanchang 330031, China

ruption will encounter the interstellar medium or dense molecular clouds around the central massive black hole, producing high-energy γ-ray afterglow through *pp* collisions (Cheng et al. 2006, 2007; Chen et al. 2015). Thus, we also search for high-energy gamma-ray emission from the normal TDE ASASSN-14li.

The analysis of the *Fermi* LAT data of TDEs is presented in Section 2. We present the result for each TDE in Section 3. Furthermore, we compare the high-energy gamma-ray emission of relativistic TDEs with that of GRB prompt emission and blazar flares. Then in Section 4, we derive constraints on the bulk motion Lorentz factor of the source based on the non-detection of the high energy emission. Finally we give a short summary. Throughout this paper, we take the standard ΛCDM cosmology with parameters $H_0 = 71$ km s^{-1} Mpc^{-1}, $\Omega_m = 0.27$, and $\Omega_\Lambda = 0.73$.

2. DATA

2.1. *γ-ray data*

The *Fermi* LAT is a pair conversion telescope designed to cover the energy band from 20 MeV to greater than 300 GeV, and operates primarily in an all-sky scanning survey mode (Atwood et al. 2009; Abdo et al. 2009). The LAT data currently being released by the FSSC (*Fermi* Science Support Center[4]) have been processed using the "Pass 8" (P8R2) event-level analysis, and specifically P8R2 source event class data are selected here. The analysis is based on the LAT science tools version v10r0p5. In order to reduce the contamination from Earth Limb emission, less than 52° of LAT rocking angle and less than 90° of local zenith angle are required. Moreover, we exclude the time period when the spacecraft is above the South Atlantic Anomaly. We perform an unbinned maximum likelihood analysis of the selected data with the following method. Front-back converting photons (evtype =3) of energies between 100 MeV and 10 GeV are fitted with a power law spectrum ($N(E) = N_0(E/E_0)^{-\Gamma}$). All events in a region of interest (ROI) of 10° have been used, and point sources and extending sources within extra 5° in the LAT 4-year Point Source Catalog (3FGL)(Acero et al. 2015) are added to the model file. The galactic diffuse and isotropic emission are molded with gll_iem_v06.fits and iso_P8R2_SOURCE_V6_v06.txt respectively. When it leaves too many free parameters to gain a good spectral fit for a faint source at a short time interval, we fix the spectral form and free the normalization ('prefactor') of faint or distant background sources.

For the purpose of comparison, we also analyze the *Fermi*/LAT data of two typical blazars, i.e. Mrk 421 and 3C 279, during some flare episodes (Bartoli et al. 2015; Hayashida et al. 2012). Analysis threads are similar to the above method. For GRBs, we select the first *Fermi* LAT GRB Catalog (Ackermann et al. 2013) as our sample for comparison with TDEs. The processing procedure for the LAT data of GRBs follows our previous work (Tang et al. 2015).

2.2. *X-ray data*

Thanks to *Swift*/BAT (Gehrels et al. 2004; Barthelmy et al. 2005), for bright X-ray sources such as the three relativistic TDEs mentioned above, we can get the daily average count rate in the survey mode (data quality flag = 0) (Krimm et al. 2013) [5] (Because Sw J1644+57 was mistaken for a GRB, it was observed by BAT burst mode and had a good follow-up observation (Burrows et al. 2011)). Considering the limited BAT energy band (15-50 keV), the corresponding flux will be displayed in the SED plot (Figure 2) as one data point.

[4] `http://fermi.gsfc.nasa.gov/ssc/data/`

3. RESULTS

3.0.1. *Sw J1644+57*

The likelihood analysis of Sw J1644+57 centered at the position (RA., Dec.)=(251.205°, 57.5810°) results in a low TS value (< 10), i.e. no significant high-energy emission is found from the BAT trigger time to one hundred days after the trigger ($T_0 + 10^7$s). Its 95% confidence upper limit fluxes are presented in Table 1 for different time intervals [6]. We fix the spectral photon index at $\Gamma = -2.0$. Taking different spectral index Γ will result in a slight, but insignificant difference. We examine the archival database day by day for three days before T_0 and yield non detection either. Our results are consistent with the results in Burrows et al. (2011), in spite of some slight difference due to new data (PASS 8), different photon index Γ and background model. The SED in 0.3-150 keV during the bright period is extracted from Burrows et al. (2011) and plotted in Figure 2. The upper limit fluence in 0.1-10 GeV is $F(0.1-10\mathrm{GeV}) \leq 6.30 \times 10^{-6}$ erg cm^{-2} during the first three days when the source is in the brightest phase in BAT.

Integrating the BAT emission over the significant emission period, we get a total 15-50 keV fluence of $1.58 \pm 0.1 \times 10^{-4}$ erg cm^{-2}, as shown in Table 2. In order to compare with GRBs, whose fluences are given in the *Fermi* Gamma-ray Burst Monitor (GBM) band (10-1000 keV), we adopt a power law spectrum with an index -2.15 ($N(E) = N_0(E/E_0)^{-2.15}$) to extrapolate the 15-50 keV fluence to the 10-1000 keV range[7], resulting in a 10-1000 keV fluence of about 5.06×10^{-4}erg cm^{-2}. One can see that the X/γ-ray fluence is about two orders of magnitude larger than that in 0.1-10 GeV gamma-rays.

3.0.2. *Sw J2058+05*

The standard gtlike analysis of the *Fermi*/LAT data of Sw J2058+05 centered at the position (RA., Dec.)=(314.5830°, 5.2260°) gives a non detection. The upper limit fluxes from the BAT trigger time to one hundred days after trigger ($T_0 + 10^7$s), divided into three time intervals, are given in Table 1 and also shown in Figure 1. Using the BAT and LAT observational data, the SED on 23 May 2011, which is the brightest epoch in BAT, is shown in Figure 2. Sw J2058+05 has a seventeen-day activity in the BAT observation with a total fluence of $\sim 1.64 \times 10^{-3}$ erg cm^{-2} when extrapolated to the energy range of 10-1000 keV (see section

[5] `http://swift.gsfc.nasa.gov/results/transients/`

[6] LAT upper limit flux is at 95% confidence level if not explicitly specified.

[7] As there is no spectral information of TDEs in the range of 10-1000 keV, we check the difference when assuming different photon indices. Taking photon index of -1.80, -2.00, -2.15, -2.30 gives an extrapolation factor of 5.12, 3.82, 3.21, 2.79 respectively. As the spectrum gets softening towards the higher energy, as seen in Figure 2 for Sw J1644+57, we adopt -2.15 for the estimation.

3.0.1). The corresponding LAT upper limit fluence is $F(0.1-10\mathrm{GeV}) \leq 1.67\times10^{-5}$ erg cm^{-2} in the same time interval.

3.0.3. *Sw J1112-82*

The likelihood analysis of the *Fermi*/LAT data of Sw J1112-82 centered at (RA., Dec.)=(167.949°, −82.6460°) also yields a non-detection. The upper limit fluxes from the BAT trigger to one hundred days after trigger ($T_0 + 10^7$s) are given in Table 1 and also shown in Figure 1. We show the BAT and LAT data on 16 June 2011 (the brightest epoch in BAT) in the SED plot (Figure 2). The LAT upper limit fluence during the period with bright BAT emission (from 16 June 2011 to 19 June 2011) is 9.00×10^{-6} erg cm^{-2}, while the 10-1000 keV fluence in the same time interval is $\sim 9.61\times10^{-4}$ erg cm^{-2}.

3.0.4. *ASASSN-14li*

The nearest TDE discovered to date, ASASSN-14li, is centered at (RA., Dec.)=(192.063°, 17.7739°) (Jose et al. 2014). We analyze the *Fermi*-LAT data during the period from 22 November 2014 to 22 November 2015 and find no evidence of high-energy gamma-ray emission, with a low TS value (< 10). The upper limit fluxes are presented in Table 1 and also shown in Figure 1. Search for high energy gamma-ray emission from the same source in the archival data also yields only upper limit. At distance of 90 Mpc, the upper limit luminosity in 0.1-10 GeV is $L(0.1-10\mathrm{GeV}) \leq 4.40\times10^{42}$ erg s^{-1} during the period from 22 November 2014 to 17 March 2015. This limit luminosity is lower than the soft X-ray (0.1-3 keV) luminosity, which is about 10^{43}erg s^{-1} (Holoien et al. 2016). However, it is higher than the predicted gamma-ray luminosity, $10^{39}-10^{40}$ erg s^{-1}, by Cheng et al. (2007), so closer TDEs detected in future are needed to test the prediction.

3.0.5. *Comparison with GRBs and Blazars*

Since relativistic TDEs have relativistic jets similar to GRBs and blazars, we compare the GeV emission in TDEs with the other two relativistic sources. For GRBs, we make the combined GBM-LAT spectral analysis during the prompt emission period, and the data of the GeV fluence and X/γ-ray fluence are presented in Figure 3, which are consistent with the results in the *Fermi* LAT First Gamma-Ray Burst Catalog (see their Fig. 17) (Ackermann et al. 2013). For blazars, we choose Mrk 421 and 3C 279 as representatives of BL Lac objects and Flat Spectrum Radio Quasar (FSRQs) respectively. We select the time intervals that X-ray emission flares to analyze the *Fermi* LAT data (Bartoli et al. 2015; Hayashida et al. 2012). The modeling of 0.1-10 GeV spectrum of Mrk 421 with a simple power law function gives a photon index of $\Gamma > -2$, whereas it gives a soft photon index with $\Gamma < -2$ for 3C 279, which are consistent with the statistic characteristic of joint BAT-LAT spectral properties of blazars (Sambruna et al. 2009). Long-time 0.1-300 GeV data gives a preferred spectral model logarithmic parabola for 3C279 in 3FGL, so we check our result with this spectral model and find almost no difference in the fluence. The results of their X/γ-ray and GeV fluences are listed in Table 2 [8].

In Figure 3, we compare the X/γ-ray fluence and GeV fluence of the three types of relativistic sources. We find that all GRBs have GeV fluences larger than 1% of the X/γ-ray fluences. Among them, a significant fraction of GRBs have GeV fluences larger than 10% of the X/γ-ray fluence. Blazar flares have similar properties and all of them have GeV fluences larger than a few per cent of the X/γ-ray fluences. In contrast, the GeV fluences of all three relativistic TDEs are smaller than 1% of the X/γ-ray fluences. This **could be due to** that the high-energy gamma-ray emission in TDEs are highly absorbed, as we will discuss below.

4. DISCUSSIONS

The non-thermal X-ray emission in three relativistic TDEs may be produced by relativistic electrons via synchrotron radiation (Burrows et al. 2011; Wang & Cheng 2012). The size of the source is estimated to be $l' = \Gamma c t_v = 3\times10^{13}\mathrm{cm}\Gamma_1 t_{v,2}$, where Γ is the bulk Lorentz factor of the source, t_v is the variability timescale of X-ray emission and we have assumed that the jet aligns with the light of sight of the observer. Here we use c.g.s. units and the denotation $Q = 10^x Q_x$ in the paper. The observed minimum variability time of the X-ray emission in Sw J1644+17 is about $t_v = 100$s (Bloom et al. 2011; Burrows et al. 2011). Assuming that the magnetic field energy density is in equipartition with the radiation energy density, the magnetic field in the comoving frame of the source is estimated to be $B' = (8\pi\epsilon_B L_X/4\pi l'^2\Gamma^4 c)^{1/2} = 3\times10^3\mathrm{G}\,\epsilon_B^{1/2}L_{X,48}^{1/2}\Gamma_1^{-3}t_{v,2}^{-1}$, where ϵ_B is the equipartition factor. For such a magnetic field, the X-ray photons with frequency $\nu_X = 2\times10^{17}$Hz are produced by relativistic electrons with Lorentz factors of $\gamma_e = (\frac{2\pi m_e c\nu_X}{\Gamma e B'})^{1/2} \simeq 1.5\times10^3\Gamma_1\epsilon_B^{-1/4}L_{X,48}^{-1/4}t_{v,2}^{1/2}$. For these electrons, we expect an inverse-Compton (IC) component peaking at $h\nu_{IC} \simeq 2\gamma_e^2 h\nu_X \simeq 5$GeV when other parameters are taken with typical values. The IC flux should be comparable to or larger than that of the synchrotron component if $\epsilon_B \lesssim 1$, thus we would expect a GeV component with a luminosity of $L_{\mathrm{GeV}} \gtrsim L_X \sim 10^{48}$ erg s^{-1}. The non-detection of such a high-energy component can be attributed to a high absorption opacity due to low-energy photons in the source, i.e. the $\gamma\gamma$ absorption optical depth should be $\tau_{\gamma\gamma}(5\mathrm{GeV}) \geq 1$. The optical depth for $\gamma\gamma$ absorption is given by $\tau_{\gamma\gamma} = \sigma_{\gamma\gamma} n_t' l'$, where $\sigma_{\gamma\gamma} = (1/16)\sigma_{\mathrm{T}}$ is the cross section for $\gamma\gamma$ absorption (σ_{T} is the Thompson cross section) and n_t' is the comoving-frame number density of the target photons that interact with high-energy photons. For high energy photons with energy $E_h = 5$GeV, the energy of the target photons is $\varepsilon_t \gtrsim 2(\Gamma m_e c^2)^2/E_h = 10\mathrm{keV}\Gamma_1^2(E_h/5\mathrm{GeV})^{-1}$. For a power-law spectrum with a photon index of $\beta = 2$ (Burrows et al. 2011), the number density of target photons is $n_t' \simeq L_X/(4\pi l'^2\varepsilon_t' c\Gamma^4)$, where $\varepsilon_t' = \varepsilon_t/\Gamma$. One can derive an upper limit on the bulk Lorentz factor from the

[8] The SED is different for different blazars and different flare states of a source, thus a simple extrapolation factor ($N(E) = N_0(E/E_0)^{-2.15}$) may not be appropriate, but anyway, a few times change of X/γ-ray (10-1000 keV) fluence will not make the fluence ratio below 1% in Figure 3.

condition $\tau_{\gamma\gamma} \geq 1$, i.e.

$$\Gamma \lesssim \left(\frac{\sigma_{\gamma\gamma} L_X}{4\pi c^2 t_v \varepsilon_t}\right)^{1/4} = 30 L_{X,48}^{1/4} t_{v,2}^{-1/4} \left(\frac{\varepsilon_t}{10\mathrm{keV}}\right)^{-1/4}. \quad (1)$$

This shows that the bulk Lorentz factors in TDEs are much lower than that of GRBs (Lithwick & Sari 2001; Tang et al. 2015), and may even be lower than that of some blazars (Savolainen et al. 2010; Wu et al. 2016). There are other possibilities leading to non-detection of high energy emission from these relativistic TDEs, such as cut-off in the spectrum of accelerated electrons or a cooling break in the SED. More multi-wavelength observations during flaring states will be helpful to diagnose these different assumptions.

5. CONCLUSIONS

We searched for the high-energy gamma-ray emission from TDEs with the *Fermi* LAT survey data, including three TDEs confirmed with relativistic jets (Sw J1644+57, Sw J2058+05, Sw J1112-82) and a nearby normal TDE ASASSN-14li. No significant emission is found from these TDEs during the period from the *Swift*/BAT trigger time (or the inferred disruption time) to about one hundred days later. Compared with the bright non-thermal X-ray emission, the non-detection of high-energy emission in three relativistic TDEs implies that high energy emission is seriously suppressed, possibly due to the $\gamma\gamma$ attenuation by soft photons in the source. Then, we derive upper limits on the bulk Lorentz factors by assuming $\tau_{\gamma\gamma} > 1$ for relativistic jets in TDEs. The non-detection of high-energy emission from the normal TDE ASASSN-14li gives an upper limit of $L(0.1-10\mathrm{GeV}) \leq 4.4\times10^{42}\mathrm{erg\ s^{-1}}$ during the first 10^7 s after the disruption, which is already lower than the X-ray luminosity (Holoien et al. 2016), but still higher than the predicted gamma-ray luminosity (Cheng et al. 2007).

ACKNOWLEDGMENTS

This work made use of data supplied by the UK Swift Science Data Center at the University of Leicester, and Swift/BAT transient monitor results provided by the Swift/BAT team. We thank Jin Zhang for helpful discussion. This work is supported by the 973 program under grant 2014CB845800, the NSFC under grants 11273016 and 11033002, and the Excellent Youth Foundation of Jiangsu Province (BK2012011).

REFERENCES

Abdo, A. A., Ackermann, M., Ajello, M., et al. 2009, Astroparticle Physics, 32, 193
Acero, F., Ackermann, M., Ajello, M., et al. 2015, ApJS, 218, 23
Ackermann, M., Ajello, M., Asano, K., et al. 2013, ApJS, 209, 11
Alexander, K. D., Berger, E., Guillochon, J., Zauderer, B. A., & Williams, P. K. G. 2015, arXiv:1510.01226
Atwood, W. B., Abdo, A. A., Ackermann, M., et al. 2009, ApJ, 697, 1071
Barthelmy, S. D., Barbier, L. M., Cummings, J. R., et al. 2005, Space Sci. Rev., 120, 143
Bartoli, B., Bernardini, P., Bi, X. J., et al. 2015, arXiv:1511.06851
Bloom, J. S., Giannios, D., Metzger, B. D., et al. 2011, Science, 333, 203
Brown, G. C., Levan, A. J., Stanway, E. R., et al. 2015, MNRAS, 452, 4297
Burrows, D. N., Kennea, J. A., Ghisellini, G., et al. 2011, Nature, 476, 421
Cao, D., & Wang, X.-Y. 2012, ApJ, 761, 111
Cenko, S. B., Krimm, H. A., Horesh, A., et al. 2012, ApJ, 753, 77
Chen, X., Gómez-Vargas, G., & Guillochon, J. 2015, arXiv:1512.06124
Cheng, K. S., Chernyshov, D. O., & Dogiel, V. A. 2007, A&A, 473, 351
Cheng, K. S., Chernyshov, D. O., & Dogiel, V. A. 2006, ApJ, 645, 1138
Gehrels, N., Chincarini, G., Giommi, P., et al. 2004, ApJ, 611, 1005
Hayashida, M., Madejski, G. M., Nalewajko, K., et al. 2012, ApJ, 754, 114
Holoien, T. W.-S., Kochanek, C. S., Prieto, J. L., et al. 2016, MNRAS, 455, 2918
Jose, J., Guo, Z., Long, F., et al. 2014, The Astronomer's Telegram, 6777,
Komossa, S. 2015, Journal of High Energy Astrophysics, 7, 148
Krimm, H. A., Holland, S. T., Corbet, R. H. D., et al. 2013, ApJS, 209, 14
Krimm, H. A., Kennea, J. A., Holland, S. T., et al. 2011, The Astronomer's Telegram, 3463,
Krimm, H. A., Kennea, J. A., Holland, S. T., et al. 2011, The Astronomer's Telegram, 3384,
Levan, A. J., Tanvir, N. R., Cenko, S. B., et al. 2011, Science, 333, 199
Lithwick, Y., & Sari, R. 2001, ApJ, 555, 540
Liu, D., Pe'er, A., & Loeb, A. 2015, ApJ, 798, 13
Lodato, G., Franchini, A., Bonnerot, C., & Rossi, E. M. 2015, Journal of High Energy Astrophysics, 7, 158
Metzger, B. D., Giannios, D., & Mimica, P. 2012, MNRAS, 420, 3528
Rees, M. J. 1988, Nature, 333, 523
Sambruna, R. M., Donato, D., Ajello, M., Maraschi, L., & the GSFC BAT Team 2009, arXiv:0912.2721
Savolainen, T., Homan, D. C., Hovatta, T., et al. 2010, A&A, 512, A24
Tang, Q.-W., Peng, F.-K., Wang, X.-Y., & Tam, P.-H. T. 2015, ApJ, 806, 194
van Velzen, S., Anderson, G. E., Stone, N. C., et al. 2015, arXiv:1511.08803
Wang, F. Y., & Cheng, K. S. 2012, MNRAS, 421, 908
Wang, J.-Z., Lei, W.-H., Wang, D.-X., et al. 2014, ApJ, 788, 32
Wu, Q., Zhang, B., Lei, W.-H., et al. 2016, MNRAS, 455, L1
Zauderer, B. A., Berger, E., Soderberg, A. M., et al. 2011, Nature, 476, 425

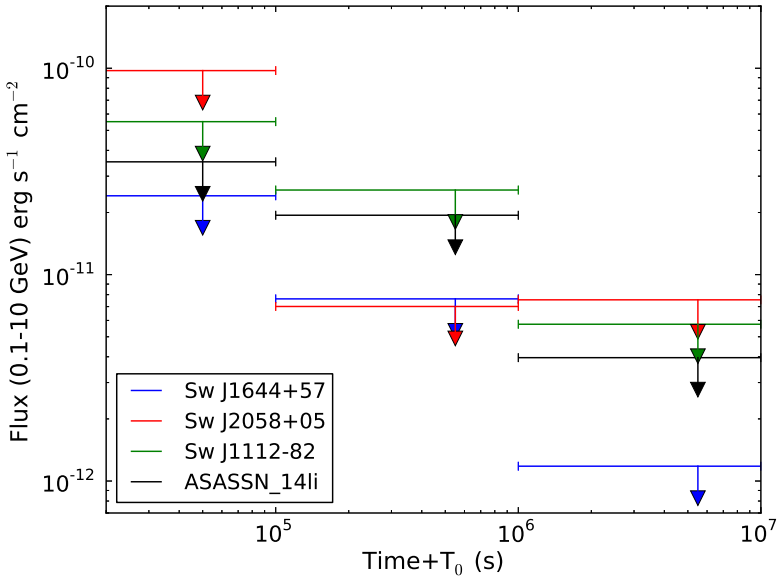

FIG. 1.— *Fermi*/LAT (0.1-10 GeV) light curves of four tidal disruption events. The upper limits are at the 95% confidence level.

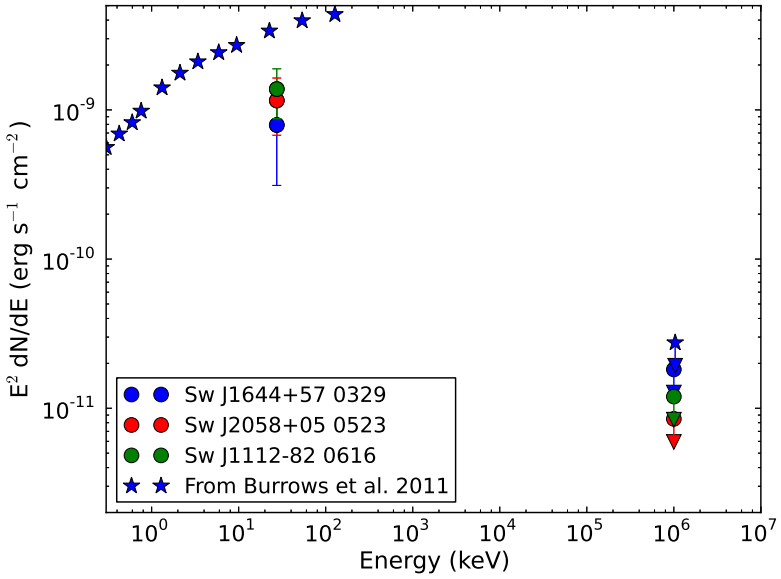

FIG. 2.— The spectral energy distribution of three relativistic tidal disruption events. The legend "Sw J1644+57 0329" means the spectrum on 29 March 2011. Data marked with blue stars are taken from Burrows et al. (2011).

TABLE 1
Fermi LAT UPPER LIMIT FLUX (95% CONFIDENCE LEVEL) OF FOUR TIDAL DISRUPTION EVENTS AT THREE TIME INTERVALS AFTER THEIR TRIGGER TIME. FLUX IS IN UNIT OF ERG CM^{-2} S^{-1} (0.1-10 GEV).

Name	Γ	Time s	Flux 10^{-11}	Time s	Flux 10^{-12}	Time s	Flux 10^{-12}
Sw J1644+57	2.0	0-10^5	2.41	10^5-10^6	7.63	10^6-10^7	1.18
Sw J2058+05	2.0	0-10^5	9.74	10^5-10^6	7.01	10^6-10^7	7.55
Sw J1112-82	2.0	0-10^5	5.51	10^5-10^6	25.7	10^6-10^7	5.75
ASASSN_14li	2.0	0-10^5	3.52	10^5-10^6	19.4	10^6-10^7	3.96

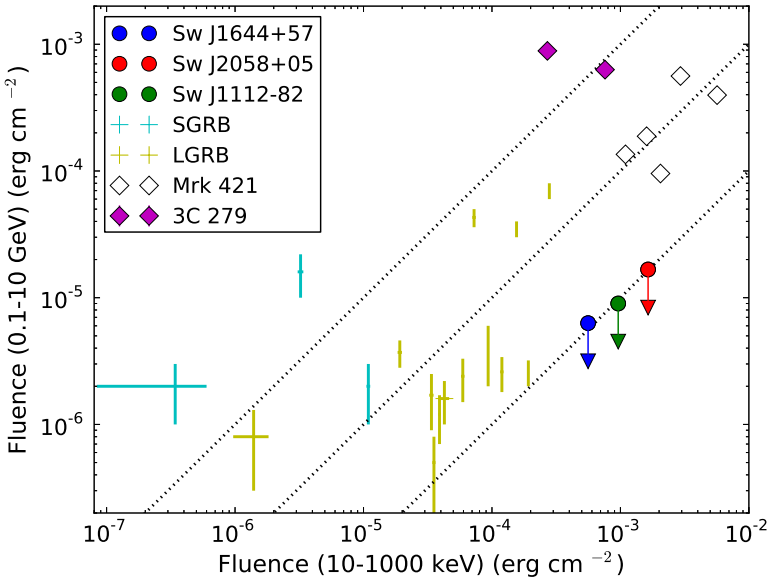

FIG. 3.— Fluence measured by *Fermi* LAT vs. the fluence measured by *Swift*/BAT or *Fermi*/GBM during the X/γ-ray flare periods for relativistic sources: TDEs, GRBs and blazars. SGRB and LGRB mean short GRB and long GRB respectively. The three dished lines from left to right denote the 100%, 10%, and 1% fluence ratio between 0.1-10 GeV and 10-1000 keV.

TABLE 2
FLUX/FLUENCE OF THREE TDES AND TWO BLAZARS DURING THEIR FLARE STATES. THE UNIT OF FLUX IS 10^{-8} PH CM^{-2} S^{-1}, AND THE UNIT OF THE FLUENCE IS 10^{-6} ERG CM^{-2}.

	MJD day	Γ 0.1-10 GeV	Fluence 0.1-10 GeV	Fluence 15-50 keV	Fluence 10-1000 keV
Sw J1644+57	55648-55650	2.0	< 6.3	157.7 ± 10.0	506
Sw J2058+05	55698-55714	2.0	< 16.7	511.6 ± 118.3	1642
Sw J1112-82	55728-55731	2.0	< 9.0	299.2 ± 65.7	961
Mrk 421	55144-55149	1.57 ± 0.21	95.5 ± 19.9	638.6 ± 59.3	2050
	55242-55245	1.46 ± 0.13	135.3 ± 24.3	341.0 ± 14.7	1095
	55246-55272	1.81 ± 0.08	397.0 ± 36.1	1761.8 ± 48.9	5655
	55475-55503	1.79 ± 0.06	561.6 ± 41.9	914.1 ± 68.2	2934
	55811-55818	1.75 ± 0.11	188.2 ± 27.0	498.0 ± 47.0	1599
3C 279	54920-54980	2.37 ± 0.03	631.1 ± 6.94	236.4 ± 116.5	759
	55030-55050	2.30 ± 0.01	886.7 ± 9.66	84.9 ± 68.0	273